A Study of Isothermal Mechanical Fatigue of Welded Reactor Steel (15H2MFA)

Degu Fedesa Keba

Ashokkumar Thanganadar (ntashoknt.1966@gmail.com)

Institute of Technology, Haramaya University,

A. H. Abishini

Research Article

Keywords: Nuclear Power Plant, Reactor pressure vessel, 15H2MFA

Posted Date: February 17th, 2022

DOI: https://doi.org/10.21203/rs.3.rs-1345255/v1

Abstract

In material science and engineering the fatigue of metal is quite difficult to deal with and that of welded joint is an even more complex phenomenon. This complexity arises from different main factors: thermal cycles during welding, which will strongly affect the base material and induce residual stresses and distortion, the fusion process with the filler metal leads to heterogeneity to microstructure which will affect or change the original mechanical properties and chemical composition through out of the welded joint. In this study isothermal mechanical fatigue of welded reactor steel has been contemplated. The samples of the welded joint have used in this study is 15H2MFA steel type of VVER-440 reactor pressure vessel operating at Paks Nuclear Power Plant, Hungary. The reactor vessel is made of low-alloy heat resistant steel and austenitic steel with a corrosion-resistant inner (clad) surface. Reactor pressure vessel (RPV) made of 2 ¼ Cr -1Mo-V bainitic steel having a good mechanical strength and creep resistance.

1. Introduction

Unexpected age-related degradation of the mechanical properties of the RPV steel can lead to safety concerns related to the mechanisms involved in ageing, which will help later in life extension process, these mechanisms include: Fatigue, Irradiation embrittlement, Thermal ageing, Temper embrittlement, Corrosion; where attempt of study focuses on fatigue, isothermal fatigue of welded joints of reactor pressure vessel of 15H2MFA steel type. In this study thermo-mechanical fatigue experiments took place for 15H2MFA using GLEEBLE-3800 physical simulator at isothermal condition, 260°C where the test is conducted under uniaxial tension-compression loading with total strain control to investigate its fatigue life. The low cycle isothermal fatigue results were evaluated with the Coffin Manson law; the behaviour of fracture surfaces was observed using Scanning Electron Microscope (SEM). Nuclear power plant is one of the clean energies have today in the world however it is non-renewable energy; it does not have a single impact on the environmental pollution. Nuclear energy now provides about 10% of the world's electricity from about 450 nuclear power reactors in operation worldwide, total 398.9 GW(e) in net installed capacity, an increase of 2.5 GW(e) since the end of 2018. In 2019 nuclear power generated almost one third of all low carbon electricity and was set to remain the second largest source of low carbon electricity after hydro power Of the operating reactors, more than 51 are Russian designed VVER (pressurized-water) types, 16 of which are VVER-440/213 (second generation VVER) reactors operating at the Paks Nuclear Power Plant (NPP). Most of these are nearing the end of their originally planned 30 years of operation (IAEA, 2019). This RPV operates at high pressure and temperature (12.3 MPa), (297°C) respectively and includes the active core of the reactor and associated pressure equipment is of paramount importance throughout the operating hours of the power plant, as their integrity ensures that radioactive media is checked and could not endanger the workers of the power plant, the residents and the environment. Therefore, a reactor pressure vessel must be able to withstand all loads resulting from the normal operating conditions of the reactor and possible malfunctioning conditions, without damage [Trampus, 2013]. The core barrel, core baffle and protective tube unit are kept from lifting under normal operating conditions by their weight plus hold-down assemblies employing elastic components made of thermo-

expanded graphite. This performs better than the materials used in the V-320 reactor (VVER-1200), with a service life of at least four years without replacement [Rosatom, 2018]. The fatigue phenomenon in welded connections, which significantly affects the useful life of metallic structures, is an important case study in the field of structural engineering. This phenomenon is induced by cyclic loadings able of causing the failure of a structural element at minor stress levels compared to the strength limit of the material itself [(Pang et. al., 2018), (Ye et. Al., 2019), (Liu et. al., 2019), (Luo et. al., 2019), (Alencar et. al., 2019), (Alencar et. al., 2021)]. Recurring thermal cycling (during start-up/shut-down and reactor trip conditions) in combination with mechanical loadings could lead to the build-up of thermomechanical fatigue (TMF) damage in components bare to elevated temperatures under service. Generally, isothermal low cycle fatigue (IF) tests performed at the maximum temperature (*T*max) of reactor operation, are used to assess the performance of materials subjected to TMF loadings, owing to the simplicity associated with the former. However, thermal cycling in association with mechanical deformation has been reported to be more damaging compared to the isothermal mechanical strain cycling even at the *T*max of the TMF cycles [(Okazaki et al, 2003), (Jaske, 2003), (Nagesha et al, 2010), (Cheng et al, 1973), (Suresh Kumar et al, 2019), (Beck et al, 1997), (Fekete et al, 2015)] .

2. Experimental

2.1 Critical examination of a metal block containing a seam

The welding seam used in the experimental work is illustrated in Fig. 1. The piece was made at the reactor vessel manufacturing plant at Skoda Power Plant in Plzen at the same time as the Paks reactor vessels were manufactured.

The material shown is 140 mm thick Cr-Mo-V alloy steel with ferrite structure which, after forging, is heat-treated to a state of precipitation hardening. This material state is stable in terms of durable mechanical and heat demand. The arrow-marked side is provided with titanium-stabilized chrome-nickel alloy corrosion-resistant cladding.

Tables 1 and 2 shows the approximate chemical composition and mechanical properties of the steel 15H2MFA,respectively.

Table 1
Chemical composition of test materials- 15H2MFA (welded joints of RPV)

Material	Composition [%]
C	0.13–0.18
Si	0.17–0.37
Mn	0.30–0.60
S	Max.0.025
P	Max.0.025
Cr	2.50-3.00
Ni	Max.0.040
Mo	0.60–0.80
V	0.25–0.35
As	Max.0.05
Co	Max.0.02
Cu	Max.0.015

Table 2
.Mechanical properties of test materials 15H2MFA (welded joints of RPV) at 20°C and 350°C

Materials	Mechanical Properties
Temperature at 20°C	
Tensile strength [MPa]	540
Yield strength [MPa]	431
Elongation [%]	14
Reduction area [%]	50
Temperature at 350°C	
Tensile strength [MPa]	490
Yield strength [MPa]	392
Elongation [%]	13
Reduction area [%]	50

The specimen is characterized by the fact that it has a welding seam in its entire cross-section. Prior to the preparation of the specimens, a macro-metallographic examination of the weld of the sample is carried out, for which the specimen is prepared as follows:

- Cutting the work-piece at the points marked with a red line in the picture taking care to mark the machining position with a pin on the surface of the work-piece.
- Planning and grinding of the surface marked with red arrow (cross section of weld seam), preparation for macro metallographic etching.
- Polishing the surface marked with a red arrow in several steps, finishing with a sanding cloth of 1200, then polishing.
- Development of polished surface fabric structure with 8% Nital etching agent. Figure 2 below shows the result of metallographic etching. The figure shows the structure of the multilayer, sealed seam, and the heat effect zone, as illustrated in the Fig. 3. Having a macro metallographic image, It can determine the exact location of the specimens to be machined.

A schematic diagram of the welded joint is shown in Fig. 4

In addition to knowing the structural homogeneity of the suture, the homogeneity of the composition of the seam is essential to determine the number of specimens required for the fatigue tests. To determine the alloy content distribution along the seam, a numerical sampling at the locations indicated in Fig. 4 was performed for composition analysis. Composition testing was performed at Dunaferr Zrt's Metallographic Laboratory using ICP-OES composition testing equipment. The test required 5g of chips, which were obtained by drilling with 12 to 15mm deep perpendicular borehole drill bit.

Based on the measurement results conducted it can be shown that the weld seam has a uniform distribution across its entire cross-section except for the first fill line.

2.2 Determination of typical dimensions of test specimens

Based on the above data and bearing in mind the sample geometry required by the GLEEBLE 3800 simulator described above, the dimensions of the fatigue specimen required for testing were determined. There is limited space in the physical simulator chamber, which should be considered when designing the specimens. The specimens shall be compatible with the clamping system of the equipment and shall withstand the high compressive stresses without bending. The specimens formed are exhibited cracks at the transition between the cylindrical section and the rounding, which is one of the disadvantageous resulted due to the resistance heating and heat removal of the clamping jaws, a slightly decreasing temperature distribution in the specimen is axially decreasing to the two sides of the thermocouple providing the control signal, so that damage at the desired radius does not occur. By modifying the geometry of the specimen, it was necessary to ensure that the cracks in the cylindrical section were formed with, certainty. By modifying the geometric model, it has been demonstrated that using a 10 mm radius reduces this effect to the desired level, so the dimensions of the specimen has been modified and

made further test measurements. It is clearly visible that each of the 10 mm rounded specimens had a crack in the middle third of the cylindrical section, as shown in Fig. 6

The samples used for the experiment are made of 13 mm edge-length square column prefabricated on the CNC lathe. Before the start of the tests, all samples have been polished to the same surface grade on conventional lathes to minimize the impact of the surface irregularity from production on the wearable test results. The 2D geometry of the sample is been shown in Fig. 7

2.3 Manufacture of test specimens

Based on the specimen enclosure dimensions and the size of the welded block, the welding splitting plan is determined as shown in Fig. 8. Cutting of the weld block started with the knowledge of the finished cutting plan shown in the Fig. 10 below and the fabric image of the seam shown above (Fig. 9).The completed specimens are shown in Figs. 9–13.

The eighty pieces of samples were prepared by marking their exact location with an (X, Y) coordinate and for those that their position in the seam can be accurately identified and manufactured as shown in the 3D drawing of the Fig. 10 below.

Barcode label is given to all samples selected for fatigue test to identify them during the operation as shown below in Fig. 11.

In the first phase of cutting, a section parallel to the weld cross-section was cut and subjected to repeated metallographic examination. The purpose of this is to make the weld contour and the heat effect zone visible and to facilitate hardness measurement (See Fig. 13).

3. Results And Discussion

3.1 The Experimental Resultsand Their Evaluation.

From the data recorded during the isothermal fatigue tests, the relation between force, temperature and time is shown using the graph below in Fig. 14. This is when strain, force, and temperature data were sampled at 100 Hz. for a 0.6% total strain load. The data presented are derived from the cyclic mechanical behavior of the fatigue tests and analyzing the measurement data, it was found that the prescribed time function of the physical quantities and the measured values showed a very good agreement for all settings.

3.2 Cyclical Mechanical Behavior of Experimental Substances

The cyclical mechanical behaviour of the material is an important factor in deformation of strained-controlled low-cycle fatigue tests. The softening or hardening at the initial stage of the tests and the intensity of these depends on the various parameters like strain, amplitude and strain rate and to

determine the voltage level at which the test is performed when entering the stable phase of the fatigue test. The extreme values of the voltages as a function of cumulative damage are shown in Fig. 15.

The cyclical mechanical behaviour of 15H2MFA material is similar to that of regular center lattice steel with similar strength. During the initial phase of the tests, it showed intense cyclic softening, followed by a secondary softening phase during the stable cycles, which lasted until the appearance of a macroscopic size crack. The appearance and propagation of the crack may be related to the starting point of the definite reduction shown in the voltage diagrams in Fig. 15.

3.3 Evaluation of Measurements by Coffin-Manson

This is also called strain-based evaluation which is predominantly used to characterize low cycle fatigue behavior of materials operating at elevated temperatures and high levels of stress that observed in power plant during operation and start up or shut down procedures .In these conditions, fatigue damage is generally caused by plastic strain which can be clearly shown by Coffin Manson law as below.

$$\epsilon_p = \epsilon_f^{'} * N_f^c$$

Here ϵ_p, plastic strain amplitude; $\epsilon_f^{'}$, fatigue ductility coefficient; N_f, cycles to failure; and c, fatigue ductility exponent.To evaluate the experimental data using the Coffin-Manson model, the amplitude value of the plastic deformation was determined per load level, and the curves for each fatigue work order are shown by regression, as shown in Fig. 16 and Coffin-Manson model's parameters of 15H2MFA are listed in Table 3.

Table 3
.Coffin-Manson model parameters of 15H2MFA

Material	$\epsilon_f^{'}$	c
15H2MFA	1.0479	-0.7375

3.4 Fractographic analysis

From the samples of 15H2MFA steels those have been undertaken isothermal fatigue test, the tested samples usually have one or more major cracks and several smaller ones. The major cracks often originated at the joint between the thermocouple and the test bar. The number of large developed cracks decreases with increasing total strain amplitude, while the number of smaller cracks grows which is the developing of fatigue cracks and these focused near the ends of the main cracks and form different branches as the number of cycles or load increases which are shown in Figs. 17 and 18. The origins of the cracks are located on the sample that had undergone fatigue test and they have got a semi oval-shape which can be clearly seen on Figs. 19 and 20. The appearance of the fracture surface is a fine grained and covered with a very fine blue oxide layer. The total length of a major cracks can extend up to 3- 4mm where striations were not so prominent, as is typical for ferrite steels and the distances of them

are very short at the beginning of the crack and become coarser with increasing crack length (Figs. 21 and 22).The distance between striations firstly rises and subsequently decreases dependent on the length of crack with increasing the total strain amplitude. In this section the selected samples allowed to be broken at the large crack that is vividly seen without using magnifying glasses appropriately without damaging the crack since the target of the study all about the formation and condition of fatigue cracks using scanning electron microscope (SEM), then by registering the code of the samples and attaching them to the SEM sample holder and inserting into SEM. In the next step the program is started from the computer and after the suitable vacuum is created the study of the samples intensely commenced. Finally, from the following pictures it can be clearly understand the formation of the development of fatigue cracks using the pictures below taken by SEM for the 15H2MFA steel of different total strain amplitude and number of cycles to failure.

3.5 Investigation of the area of fatigue crack tip of 15H2MFA steel.

4. Conclusions

The isothermal low cycle fatigue behaviors of welded joints of reactor pressure vessel steel material 15H2MFA were investigated holding isothermal temperature at 260℃ under fully reversed wholly controlled strain. The isothermal low cycle fatigue tests yielded a higher fatigue life than any other thermo mechanical testing where cyclic softening has occurred in the 15H2MFA steel during the test. Throughout this thesis it was exposed that the yet unclear nature of fatigue of the VVER pressure vessel, which is even more uncertain when it comes to fatigue on welded structures where welded components may have complex state of stresses, complicated geometries and a great variety of defects introduced during welding processes. Cracks commonly occur in engineered parts and can significantly reduce their ability to withstand load and cracks typically form around pre-existing flaws in a part. It usually starts off small and then grows during operational use. There are three stages of fatigue fracture: initiation, propagation, and final rupture when the material is incapable to withstand the load at a given cycle. It is apparent that to ensure sustainable safe operation of the aging reactor units, the detail understanding of different damage mechanisms and their effects in the structural materials of the respective nuclear power plant is significant.

Declarations

The authors declare that no funds, grants, or other support were received during the preparation of this manuscript.

References

[1] Alencar, G.; de Jesus, A.; da Silva, J.G.S.; Calcada, R. Fatigue cracking of welded railway bridges: A review. Eng. Fail. Anal. **2019**, 104, 154–176.

[2] Alencar, G.; de Jesus, A.; da Silva, J.G.S.; Calçada, R. A finite element post-processor for fatigue assessment of welded structures, based on the Master SN curve method. Int. J. Fatigue **2021**, 153, 106482.

[3] Beck T, Pitz G, Lang K H, Lahe D, Thermal-mechanical and isothermal fatigue of IN 792 CC, Mater. Sci. Eng. A 234–236 (1997) 719–722

[4] Cheng C F, Cheng C Y, Diercks D R, Weeks R W, Low cycle fatigue behaviour of types 304 and 316 stainless steel at LMFBR operating temperature, in: A.E. Carden, A.J. McEvily, C.H. Wells (Eds.), Fatigue at Elevated Temperatures, ASTM STP 520, American Society for Testing and Materials, Philadelphia, 1973, pp. 355–364.

[5] Fekete B, Kasl J, Jandova D, Joni B, Misjak F, Trampus P, Low cycle thermomechanical fatigue of reactor steels: microstructural and fractographic investigations, Mater. Sci. Eng. A 640 (2015) 357–374.

[6] IAEA-TECDOC-742, 2019, “Design basis and design features of WWER-440 model213nuclear power plants. Reference plant: Bohunice V2 (Slovakia)”.

[7] Jaske C E, Thermal-mechanical, low cycle fatigue of AISI 1010 Steel, in: D. A. Spera, D.F. Mowbray (Eds.), Thermal Fatigue of Materials and Components, ASTM STP 612, American Society for Testing and Materials, Philadelphia, 1976, pp. 170–198.

[8] Liu, N.; Xiao, J.; Cui, X.; Liu, P.; Lua, J. A continuum damage mechanics (Cdm) modeling approach for prediction of fatigue failure of metallic bolted joints. In AIAA Scitech 2019 Forum; Aerospace Research Central: Reston, VA, USA, 2019; pp. 1–11.

[9] Luo, P.; Yao, W.; Li, P. A notch critical plane approach of multiaxial fatigue life prediction for metallic notched specimens. Fatigue Fract. Eng. Mater. Struct. **2019**, 42, 854–870.

[10] Nagesha A, Kannan R, Parameswaran P, Sandhya R,. Bhanu Sankara Rao K, Vakil Singh, A comparative study of isothermal and thermomechanical fatigue on type 316 LN austenitic stainless steel, Mater. Sci. Eng. A 527 (2010) 5969–5975.

[11] Okazaki M, Take K. Kakeshi K, Yamazaki Y, Sakane M, Arai M, S. Sakurai S, Kaneko H, Harada Y, Sugita Y, Okuda T, Nonaka I Fujiyama K, Nanba K, Collaborative research on the thermomechanical and isothermal low cycle fatigue strength of Ni-base super alloys and protective coatings at elevated temperatures, in: McGaw M A, Kalluri S, Bressers J, Peteves (Eds.) S D, Thermo-mechanical Fatigue Behaviour of Materials, ASTM STP 1428, American Society for Testing and Materials, Philadelphia, 2003, pp. 180–194.

[12] Pang, J.C.; Li, S.X.; Wang, Z.G.; Zhang, Z.F. General relation between tensile strength and fatigue strength of metallic materials. Mater. Sci. Eng. A **2013**, 564, 331–341.

[13] Rosatom launches annealing technology for VVER-1000 units". World Nuclear News. 27 November 2018. Retrieved 28 November, 2018.

[14] Suresh Kumar T, Nagesha A, Kannan R, Thermal cycling effects on the creep-fatigue interaction in type 316 LN austenitic stainless steel weld joint, Int. J. Press. Vessel. Pip. (2019), https://doi.org/10.1016/j.ijpvp.2019.104009.

[15] Suresh Kumar T, Nagesha A, Sandhya R, Prakash R, Suresh Kumar R, Nagesha A, G. Sasikala G, A. Bhaduri (Eds.) A, Structural Integrity Assessment, Lecture Notes in Mechanical Engineering, Springer, Singapore, 2019, pp. 377–386.

[16] Trampus, P. A reaktortartály üzemi kérdései. 2013. in: Csom Gyula (ed.): Atomerőművek üzemtana II.4: Az energetikai atomreaktorok üzemtana. Budapest: Pauker Holding

[17] Ye, X.W.; Su, Y.H.; Jin, T.; Chen, B.; Han, J.P. Master S-N Curve-Based Fatigue Life Assessment of Steel Bridges Using Finite Element Model and Field Monitoring Data. Int. J. Struct. Stab. Dyn. **2019**, 19, 1940013.

Figures

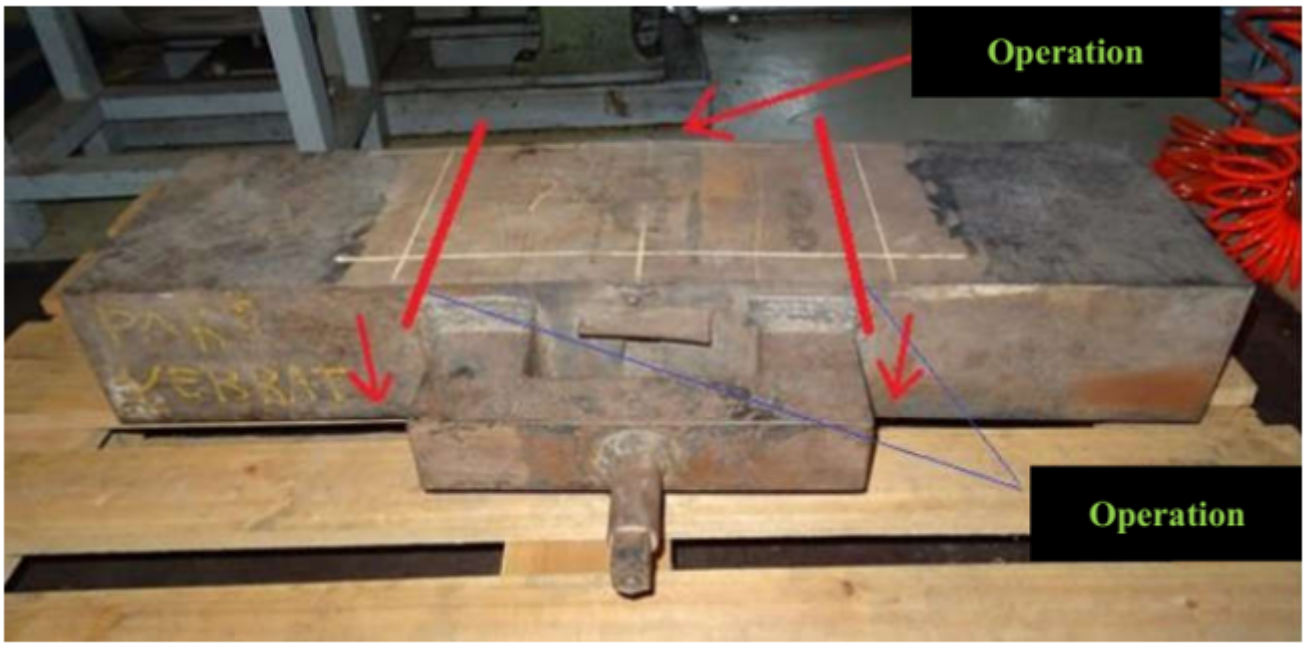

Figure 1

The raw material of specimens used for experimental work

Figure 2

Macro-metallographic image of the welded joint

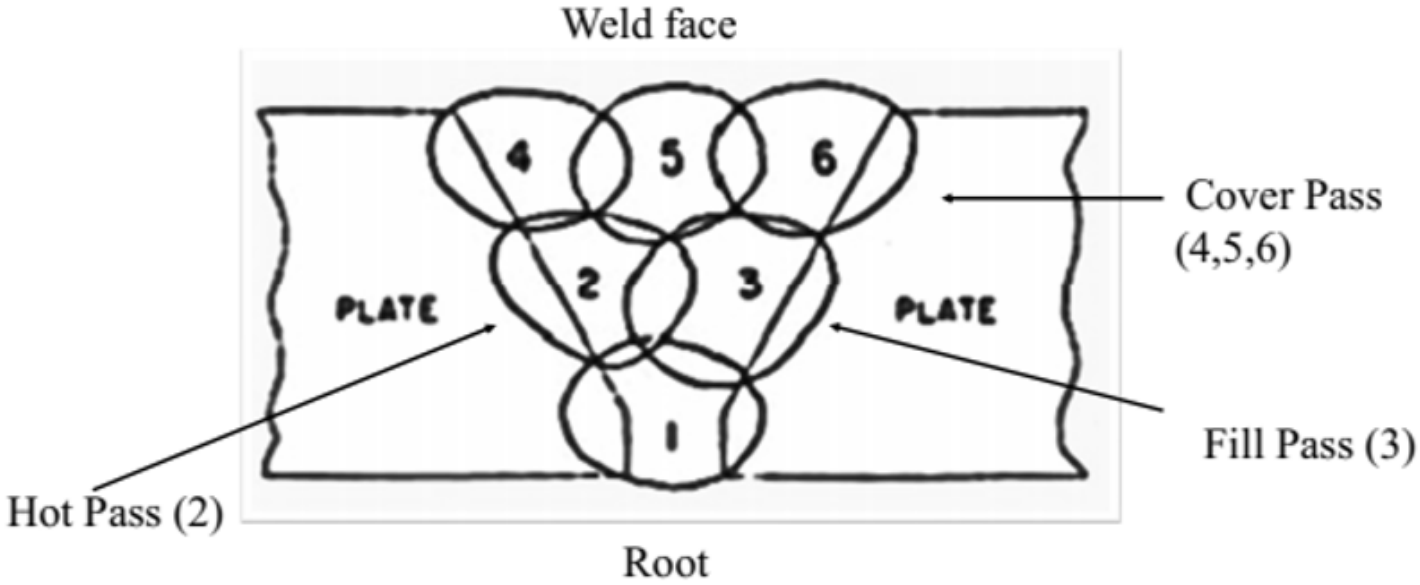

Figure 3

The structure of a multi-row seam

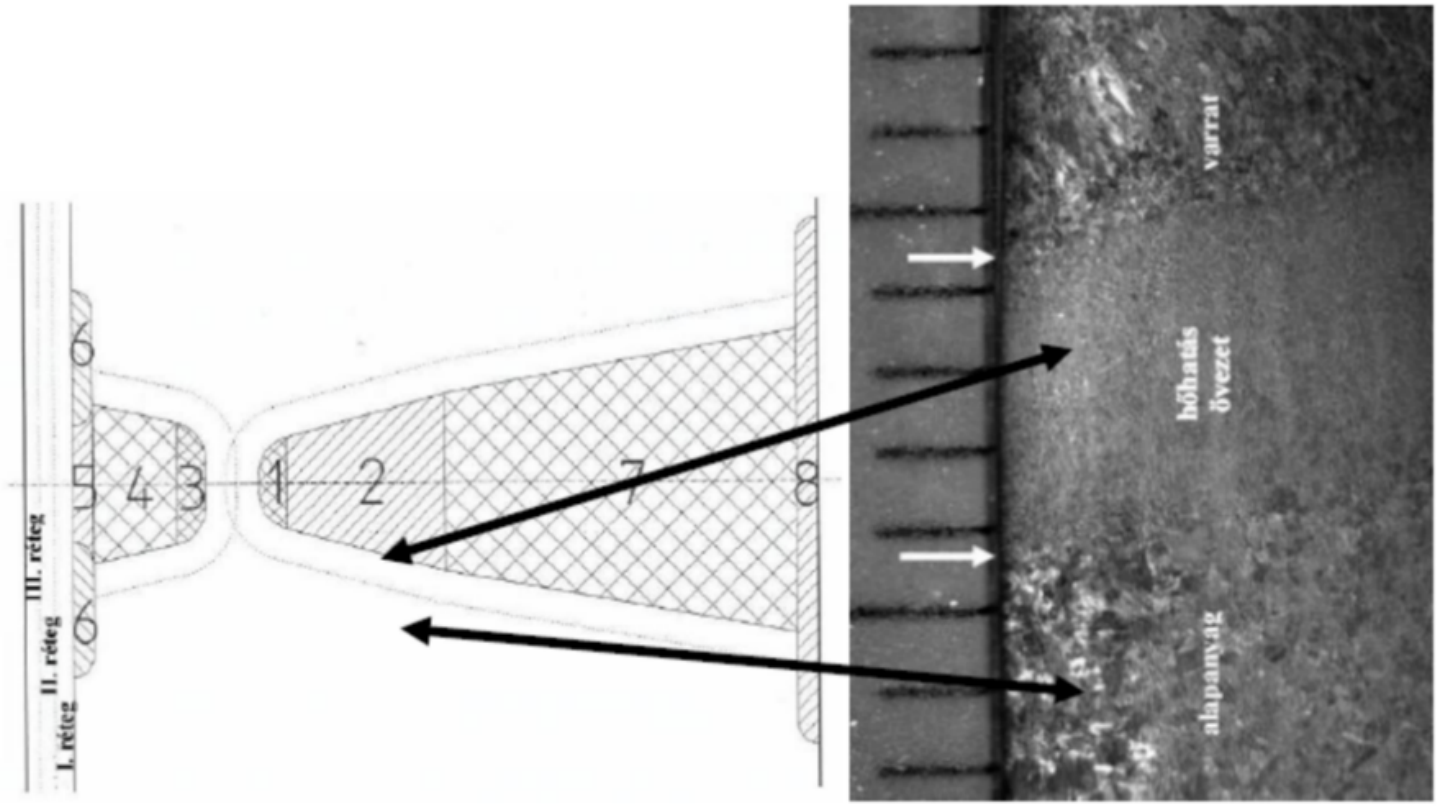

Figure 4

Schematic diagram of a welding seam of a reactor vessel

Figure 5

Position of samples for ICP-OES composition testing

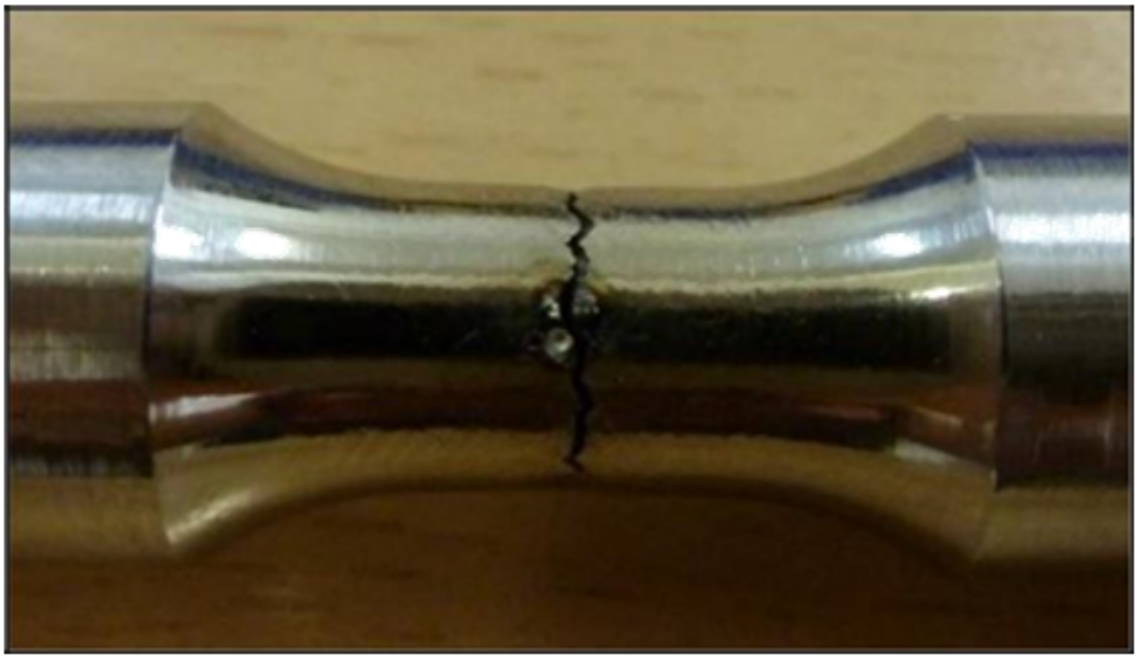

Figure 6

Test piece manufactured with 10 mm rounding after fatigue test

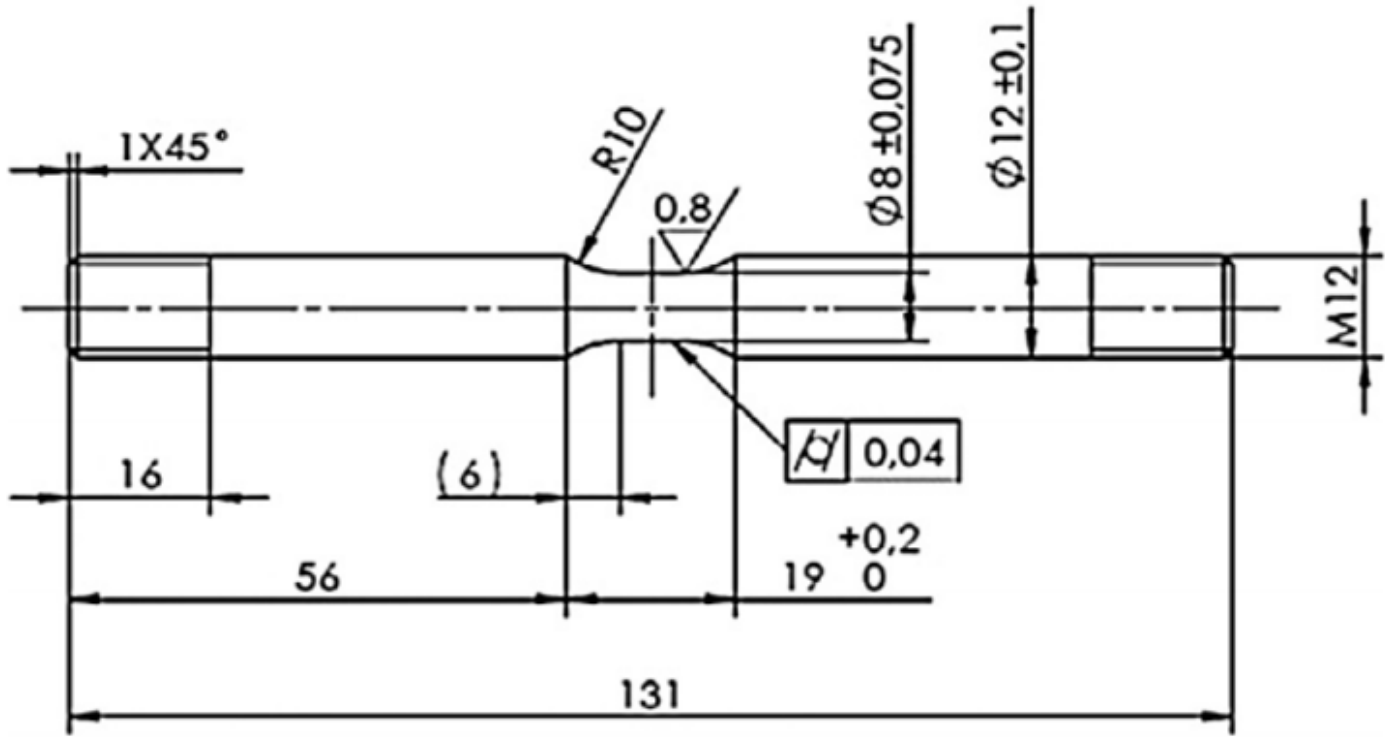

Figure 7

Dimensions of 10mm specimen required for fatigue tests

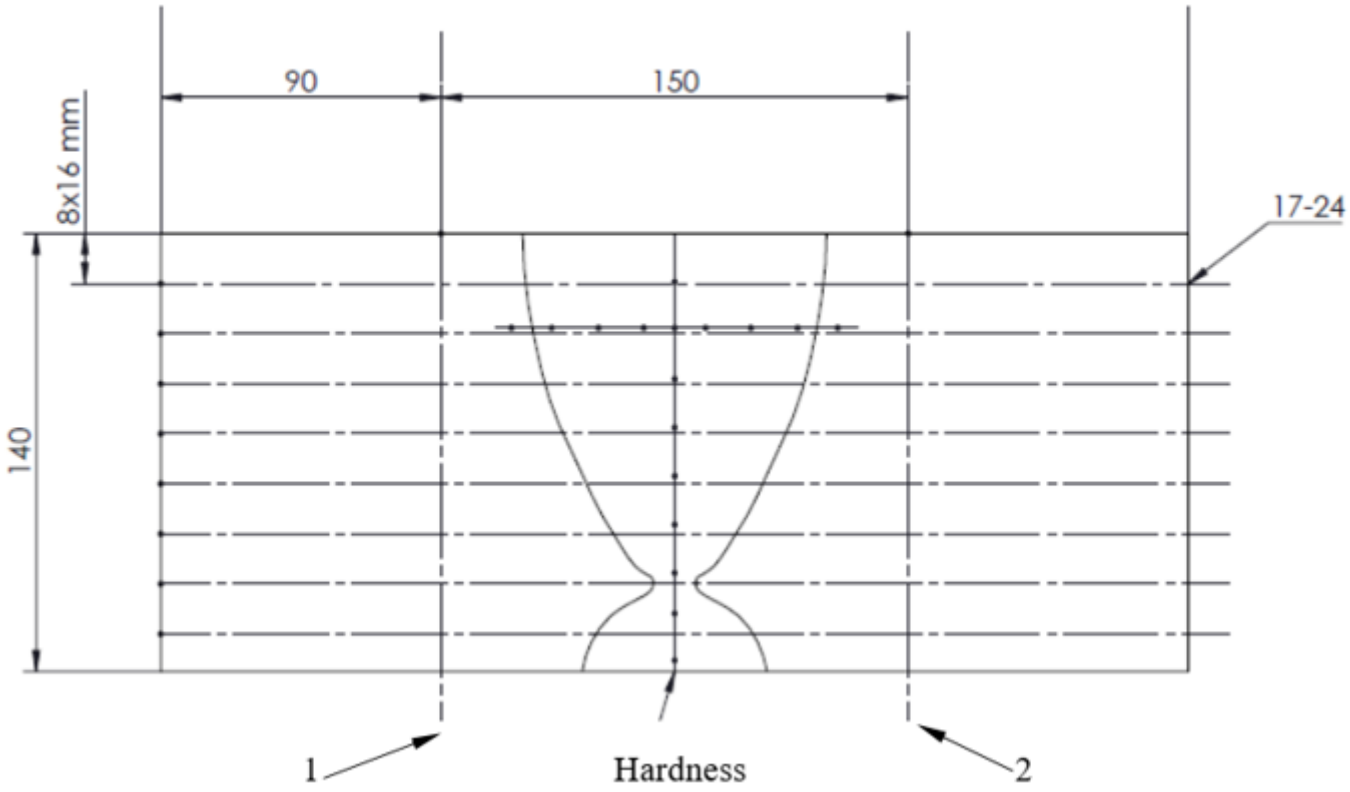

Figure 8

Cutting plan

Figure 9

Prefabricated products for turning

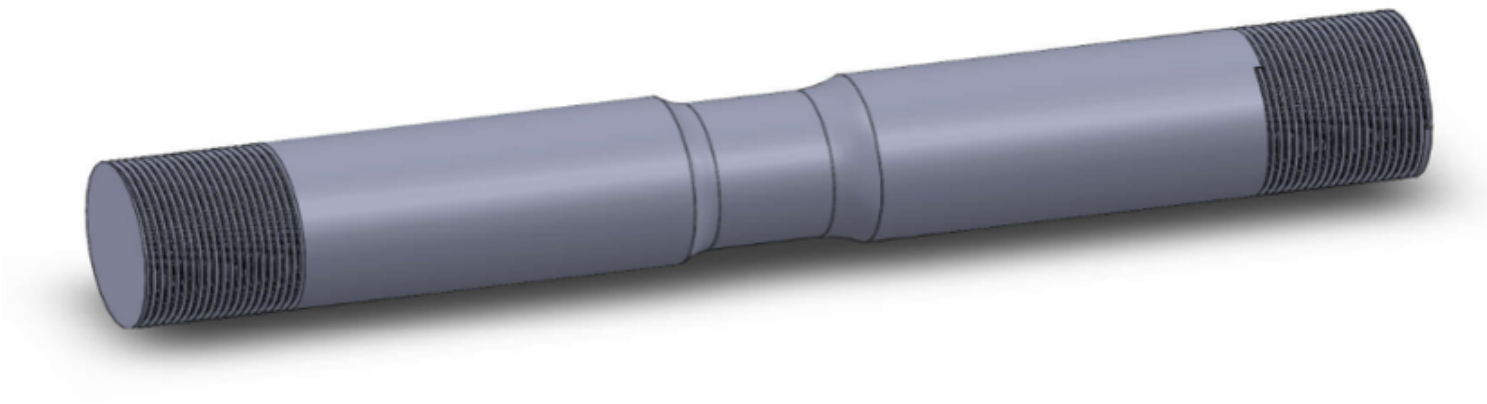

Figure 10

Drawing of the test specimen

Figure 11

Specimen with a bar-code

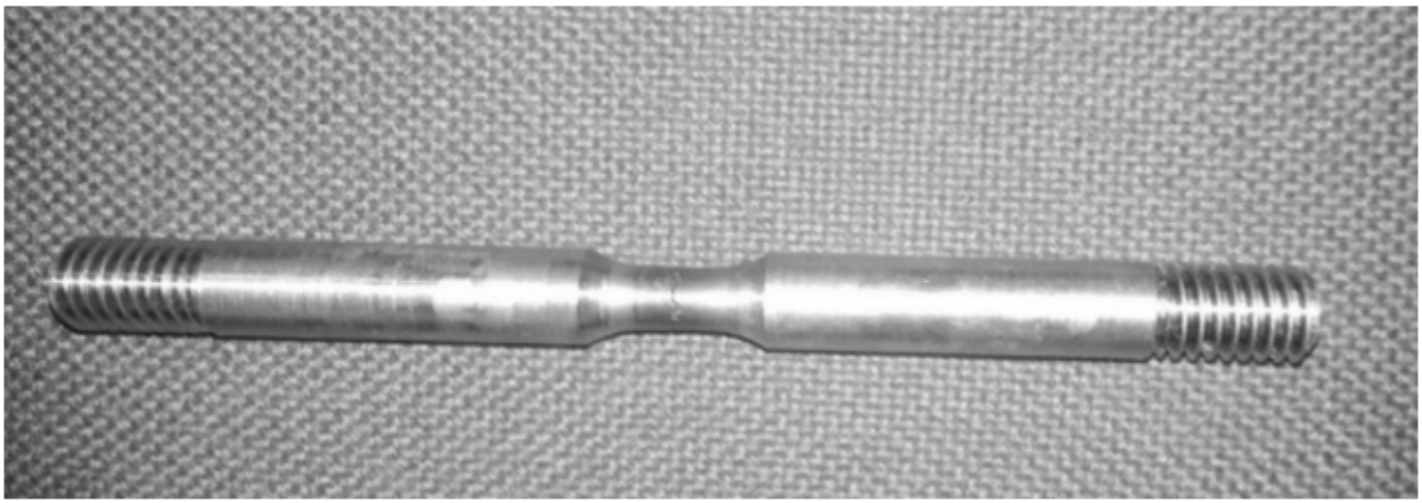

Figure 12

Turned specimen

Figure 13

Machined milled seam profile

Figure 14

Data recorded during fatigue tests. (15H2MFA, IZOT)

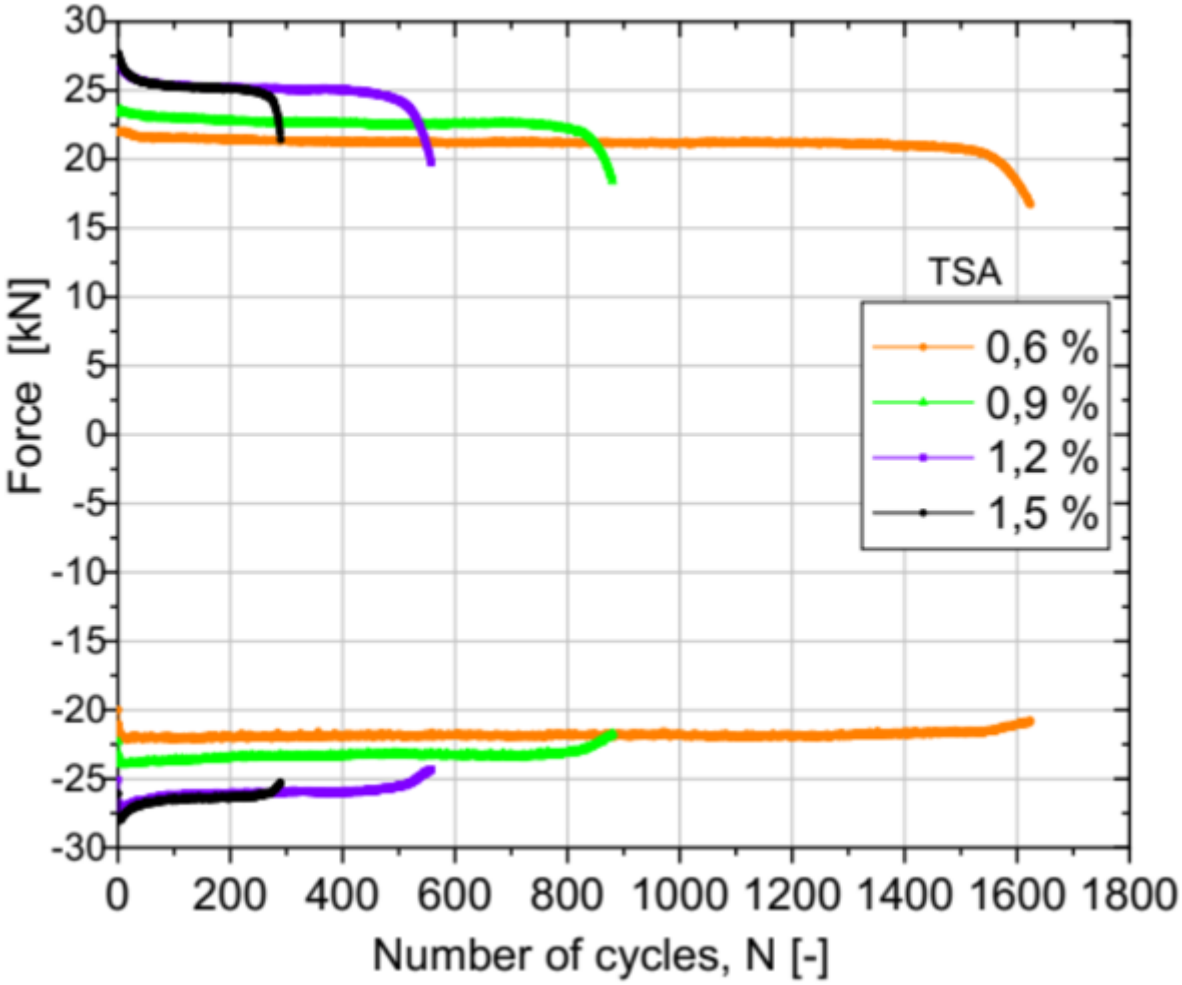

Figure 15

Extreme values of voltages recorded per cycle are 15H2MFA IZOT

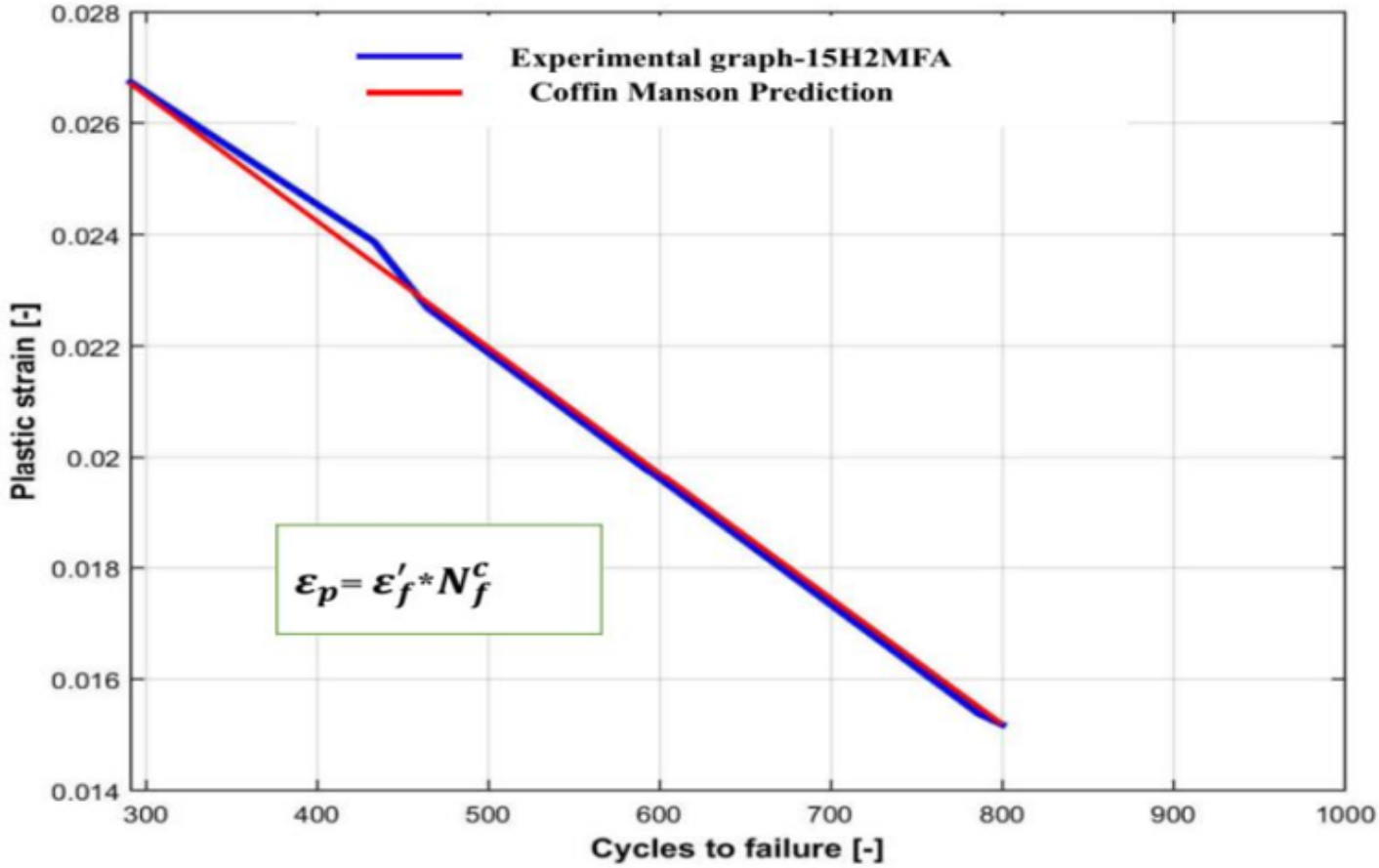

Figure 16

Coffin-Manson straight for 15H2MFA (IZOT) Seam

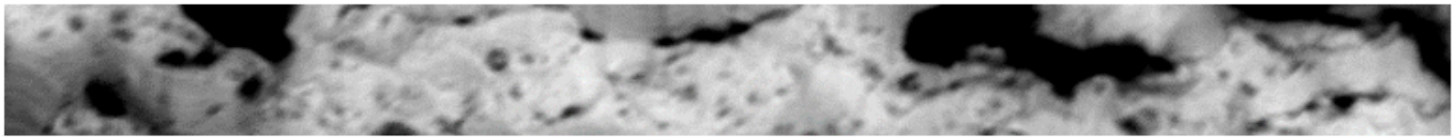

Figure 17

Fatigue crack development of test bar, ISO, N_f=380, TSA=0.9%

Figure 18

Fatigue crack development of test bar, ISO, N_f=420, TSA=1.2%

Figure 19

Fracture surface of cracks, ISO, N_f=420, TSA=1.2%

Figure 20

Fracture surface of cracks, ISO, N_f=380, TSA=0.9%

Figure 21

Fracture surface near the origin of a crack, ISO, N_f=464, TSA=1.2%

Figure 22

Fracture surface before the end of the crack, ISO, N_f=464, TSA=1.2%.